

MR Imaging of Articular Cartilage: Current State and Recent Developments

Philipp Lang, MD, MBA*, Farimah Noorbakhsh, MD,
Hiroshi Yoshioka, MD, MSc

*Division of Musculoskeletal Radiology, Department of Radiology, Brigham and Women's Hospital, Harvard Medical School,
75 Francis Street, Boston, MA 02115, USA*

Osteoarthritis (OA) is the most common type of arthritis and a frequent cause of pain and disability [1]. A number of exciting surgical treatment modalities have been introduced recently, including autologous chondrocyte transplantation [2,3] and osteochondral allografting [4,5] or autografting [6].

Conventional radiography is widely used in evaluating the long-term progression of OA and is able clearly to depict the established hallmarks of OA, namely joint space narrowing, subchondral sclerosis, subchondral cyst formation, and osteophytosis [7,8]. Conventional radiography is limited, however, by its inability directly to visualize articular cartilage, the tissue in which the earliest insults of OA are thought to occur [9]. Radiographic measurements of joint space width cannot differentiate between femoral and tibial cartilage loss and do not reveal the distribution pattern of tissue degradation throughout the joint surface [9]. Moreover, highly standardized positioning procedures and even fluoroscopic control of the exact position of the joint are required to obtain reproducible data on joint space narrowing, which is used as a surrogate measure of cartilage degeneration and disease progression [7,8].

MR imaging offers the distinct advantage of visualizing the articular cartilage directly. MR imaging can detect signal and morphologic changes in the cartilage and has been used to detect cartilage surface

fraying, fissuring, and varying degrees of cartilage thinning [10–16].

Standard MR imaging pulse sequences

The standard techniques broadly used in clinical practice and scientific studies are the two-dimensional fast spin echo (FSE) (Fig. 1) and the three-dimensional spoiled gradient-echo (SPGR) sequence [13,17]. Both sequences are available on most MR imaging systems.

Two-dimensional fast spin-echo imaging

FSE imaging affords high contrast for evaluating articular disorders and cartilage (Fig. 2) [10–13, 17,18]. Incidental magnetization transfer contrast contributes to the signal characteristics of articular cartilage on FSE images and can enhance the contrast between cartilage and joint fluid. Two-dimensional FSE sequences have excellent signal-to-noise ratios, which help to achieve short scan times in clinical practice. The sequence has fewer artifacts than three-dimensional SPGR [19]. Image blurring can be a problem in two-dimensional FSE. Strategies to decrease or avoid image blurring include the use of ultrashort echo times and short echo trains [20,21].

Three-dimensional spoiled gradient echo imaging

SPGR sequences have been used because of their ability to provide high-resolution three-dimensional images [10–12,18]. Fat suppression is typically used

This article is supported by National Institutes of Health/ National Institute of Arthritis and Musculoskeletal and Skin Diseases Grant 1 RO1 AR051873-01.

* Corresponding author.

E-mail address: pklang@partners.org (P. Lang).

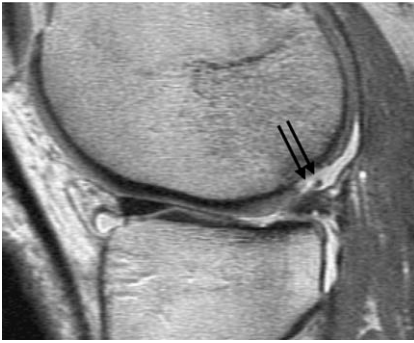


Fig. 1. Standard two-dimensional FSE pulse sequence. A sagittal MR image demonstrates the focal cartilage defect at the posterior aspect of the femoral condyle (arrows).

to increase the dynamic range of signal intensities in cartilage. The hyaline cartilage appears as a high signal intensity structure compared with adjacent tissues, which demonstrate lower signal intensities with this sequence. The three-dimensional imaging capability of this sequence has helped transform it into the standard acquisition technique for quantitative cartilage assessment, such as three-dimensional volume or thickness measurements. Recent studies indicate, however, that this sequence is hampered by significant image artifacts that can result in overestimation or underestimation of cartilage disease and failure of automated cartilage segmentation for three-dimensional analysis because of poor contrast between cartilage and surrounding tissues [22].

Many other MR imaging sequences have been proposed for cartilage imaging, but have not found widespread acceptance. These include T1-weighted [23–26], proton density weighted, and T2-weighted spin echo sequences [14,27,28]; inversion recovery sequences [29]; two- and three-dimensional magnetization transfer contrast sequences [16,30,31]; projection reconstruction spectroscopic imaging [32–34]; and two- and three-dimensional driven equilibrium Fourier transform (DEFT) [35–39]. Poor cartilage signal-to-noise (SNR) and contrast-to-noise ratios (spin echo, inversion recovery sequences), limited SNR efficiency (spin echo, inversion recovery), and need for off-line reconstruction (projection reconstruction spectroscopic imaging) or for image subtraction (magnetization transfer contrast) are among the factors that have prevented the broad dissemination and acceptance of these techniques for cartilage MR imaging.

The most promising novel MR imaging pulse sequences for cartilage imaging are water-selective excitation techniques, such as three-dimensional

SPGR with spectral spatial pulses (SS-SPGR) (ie, a water-selective excitation gradient echo sequence) [40]; three-dimensional steady-state free precession (SSFP) [35,41]; and three-dimensional FSE techniques [20,21,42]. These fast sequences hold the promise of providing three-dimensional coverage (unlike two-dimensional FSE) while yielding superior contrast-to-noise ratio between cartilage and surrounding tissues (unlike three-dimensional SPGR) and are likely to improve the accuracy and reproducibility of cartilage MR imaging.

Sensitivity and specificity of MR imaging

The sensitivity and specificity of standard MR in imaging detecting cartilage loss has been examined by correlating two-dimensional FSE or three-dimensional SPGR sequences with arthroscopic findings [10,11,13,14,17,18,43,44]. The specificity of standard two-dimensional FSE and three-dimensional SPGR sequences is excellent, ranging between 81% and 97% [10,11,14,17,18,43,44]. The data reported on the sensitivity of two-dimensional FSE [13,43] and three-dimensional SPGR [10–12,14] sequences in detecting cartilage loss are inconsistent, ranging between 60% and 94% [10,11,14,17,18,43,44].

With three-dimensional SPGR, image artifacts and a poorly defined cartilage surface contour along the posterior femoral condyle can result in false-negative or false-positive results, which may account for some of the reported variability in sensitivity. The severity of cartilage loss and the grade of OA are also important. Kawahara et al [44] reported that the



Fig. 2. Standard two-dimensional FSE pulse sequences. A sagittal MR image demonstrates diffuse, slightly less than 50% of cartilage thickness thinning along the central to posterior aspect of the medial femoral condyle (arrows). This finding is consistent with early cartilage loss in osteoarthritis.

sensitivity of two-dimensional FSE improved with higher grades of cartilage loss; the sensitivity reported in this study for superficial cartilage lesions was only 31.8%, whereas the sensitivity for full-thickness defects was greater than 90% [44]. Limited spatial resolution of the two-dimensional FSE sequence in slice direction may be the cause for this observation. Bredella et al [43] reported a sensitivity of only 61% for single-plane fat-saturated two-dimensional FSE sequences; when two or more planes were combined in the interpretation (eg, axial and coronal plane), the sensitivity increased to 93%. These data along with the limited sensitivity observed for superficial cartilage lesions in the study by Kawahara et al [44] provide a strong indication that pulse sequences with near isotropic resolution, such as three-dimensional SSFP or three-dimensional FSE, are needed to achieve sensitivities of cartilage MR imaging that are consistently greater than 90%.

Reproducibility of standard cartilage MR imaging pulse sequences

The reported reproducibility of visual readings of cartilage MR imaging acquired with a standard three-dimensional SPGR sequence is fair. In one study involving independent readings of 30 OA patients by three radiologists, the median interobserver agreement was 0.29 (range 0.06–0.38) [45]. The authors concluded that this was likely the result of errors related to partial volume averaging near the intercondylar notch and other image artifacts. This observation emphasizes the need for novel, more reproducible cartilage-sensitive imaging sequences.

Three-dimensional measurements of total cartilage volume and cartilage thickness have evolved as the standard for quantitative MR imaging-based assessment of cartilage loss [15,22,46–60]. Both measurements require segmentation of the cartilage from the surrounding tissue using such techniques as manual segmentation [15,22,52], signal intensity-based thresholding [15,52], seed-growing algorithms [53], filtering [61–63], watershed [64] and live wire approaches [54,55,65,66], or model-based segmentation [57,67–69]. Three-dimensional thickness maps can be generated using a three-dimensional Euclidean distance transformation that determines at each point the minimal distance from the articular surface to the bone-cartilage interface [46–51].

More important than accuracy is the ability to distinguish changes of cartilage volume and thickness over time, which is determined by the reproducibility of the technique. There is significant disagreement in

the literature as to the reproducibility of quantitative MR imaging-derived measurements of cartilage loss in the tibiofemoral compartments. Coefficients of variation for repeated measurements of total cartilage volume derived from standard three-dimensional SPGR sequences ranged between 1.8% and 8.2% [9,15,46,48,60,70,71], and in one study even 10% and 15% [58].

Wluka et al [72] reported that the annual rate of total tibial cartilage loss in a longitudinal study in OA patients amounted to $5.3\% \pm 5.2\%$ (mean \pm 1 SD) (95% confidence interval [CI] 4.4%–6.2%) per year, a value only slightly above most of the published reproducibility errors. The annual percentages of loss of medial and lateral tibial cartilage were $4.7\% \pm 6.5\%$ (95% CI 3.6%–5.9%) and $5.3\% \pm 7.2\%$ (95% CI 4.1%–6.6%), respectively [72]. Gandy et al [22] were not able to find any discernable change in cartilage volume in a cohort of OA patients followed with MR imaging over a 3-year period. Remarkably, radiologists' visual readings showed progression of cartilage loss in the same patients [73]. Difficulties in cartilage segmentation caused by low cartilage contrast in the three-dimensional SPGR sequence seemed to be largely responsible for the problems noted with quantitative cartilage measurements in that study [22].

Hardy et al [60] showed that the spatial resolution of the imaging sequence is of critical importance for reducing partial volume artifacts in cartilage MR imaging and for improving the reproducibility of quantitative measurements of cartilage loss. Changing the slice thickness from 1 to 0.5 mm resulted on average in a 2% decrease in coefficients of variation in the tibiofemoral compartments [60]. Similarly, a change in in-plane resolution from 0.55 to 0.275 mm caused a threefold decrease in coefficients of variation of repeated cartilage volume measurements. Alongside the high variability in published reproducibility errors [9,15,46,48,60,70,71] and the difficulties encountered by some investigators in segmenting the articular cartilage in OA patients [22,73], the results of Hardy et al [60] emphasize the need for novel three-dimensional imaging techniques with high contrast and high spatial resolution.

Image artifacts

In a recent study [19], the presence and severity of image artifacts on conventional two-dimensional FSE and three-dimensional SPGR sequences was evaluated for cartilage imaging. Four normal volunteers and 28 patients with OA of the knee (Kellgren-

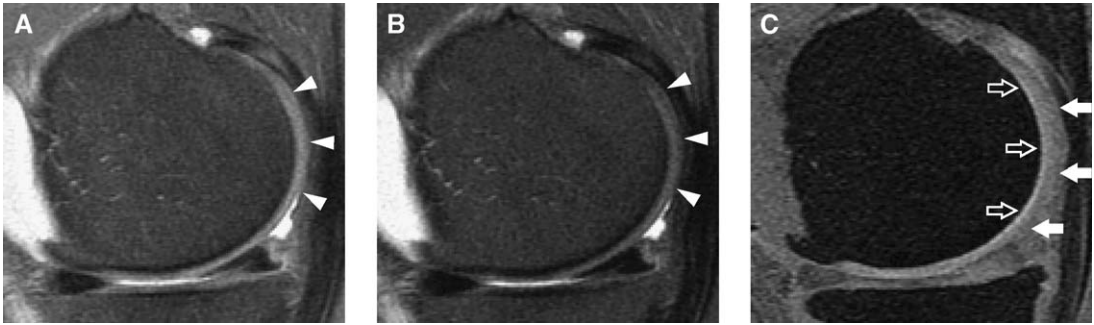


Fig. 3. Ambiguity of cartilage surface contour on three-dimensional SPGR image. MR images in a 60-year-old man. Sagittal short TE FSE image (4000/13) (A) and long TE FSE image (4000/39) with fat suppression (B) showing clearly defined cartilage contour (arrowheads) in the region of the posterior femoral condyle. (C) Sagittal fat-suppressed three-dimensional SPGR image (60/5, 40°-flip angle) shows ambiguous surface contour (arrows) on the posterior region of the femoral condyle cartilage. (From Yoshioka H, Stevens K, Genovese M, et al. Articular cartilage of knee: normal patterns at MR imaging that mimic disease in healthy subjects and patients with osteoarthritis. *Radiology* 2004;231:31–8; with permission.)

Lawrence grades I and II [74]) were prospectively studied with MR imaging (standard, conventional two-dimensional FSE [short TE and moderate TE], and three-dimensional SPGR). Imaging artifacts were noted. Signal intensities of cartilage, meniscus, joint capsule, synovial fluid, and muscle were measured and the tissue contrast was determined for each sequence [19].

The following artifacts were observed on FSE short TE, FSE long TE, and SPGR images, respectively: (1) ambiguity of the surface contour in the posterior region of the femoral condyle cartilage 0%, 0%, and 71.4% (Fig. 3); (2) linear high signal intensity in the deep zone adjacent to the subchondral bone of the femoral condyle 0%, 0%, and 92.9%; (3) pseudolaminar appearance in the posterior region of the femoral condyle cartilage 25%, 32.1%, and 85.7%; (4) truncation artifact in the patellofemoral compartment 25%, 21.4%, and 96.2%; (5) suscepti-

bility artifact on the cartilage surface caused by air or metal 10.7%, 10.7%, and 39.3%; (6) decreased signal intensity in the distal trochlear cartilage 100%, 100%, and 100%; (7) cartilage thinning in the central portion of the lateral femoral condyle adjacent to the anterior horn of the lateral meniscus 67.9%, 67.9%, and 75%; and (8) focal cartilage flattening in the posterior region of the femoral condyle 57.1%, 57.1%, and 32.1%. Limited contrast between cartilage and surrounding tissues resulted frequently in poor delineation of cartilage defects on conventional three-dimensional SPGR sequences (Fig. 4). Cartilage-meniscus contrast and cartilage-synovial fluid contrast were significantly greater on fat-suppressed two-dimensional FSE than on fat-suppressed three-dimensional SPGR images ($P < .001$) (Fig. 5).

Clearly, three-dimensional SPGR is hampered by multiple image artifacts that can obscure cartilage defects or artificially create defects [19]. These

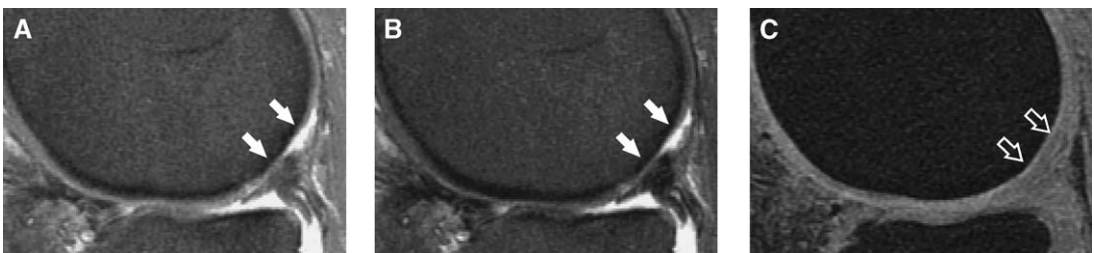


Fig. 4. Poor delineation of cartilage defect on three-dimensional SPGR sequence. MR images in the same patient seen in Fig. 2. Sagittal short TE FSE image (A) and long TE FSE image with fat suppression (B) show large, and in some areas full-thickness, cartilage defect (arrows) in the central and posterior regions of the lateral femoral condyle. (C) Although sagittal fat-suppressed three-dimensional SPGR image can demonstrate the cartilage defect, the margins are not well defined, particularly posteriorly (open arrows). The full-thickness cartilage defect was confirmed at arthroscopy. (From Yoshioka H, Stevens K, Genovese M, et al. Articular cartilage of knee: normal patterns at MR imaging that mimic disease in healthy subjects and patients with osteoarthritis. *Radiology* 2004;231:31–8; with permission.)

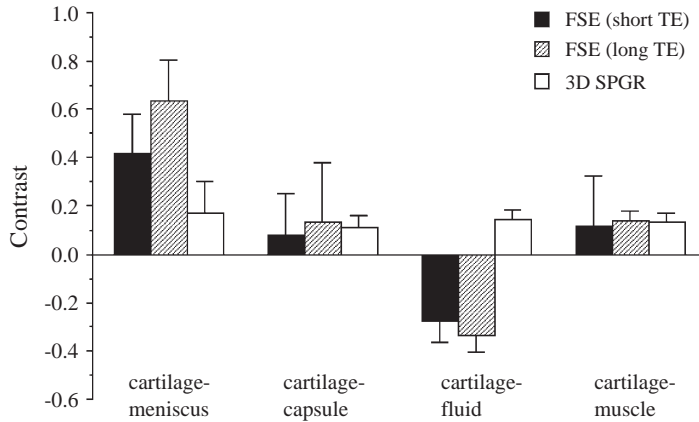


Fig. 5. Mean contrast between cartilage and adjacent structures for fat-suppressed FSE (short and long TE) images and fat-suppressed three-dimensional SPGR images. (From Yoshioka H, Stevens K, Genovese M, et al. Articular cartilage of knee: normal patterns at MR imaging that mimic disease in healthy subjects and patients with osteoarthritis. *Radiology* 2004;231: 31–8; with permission.)

artifacts along with the poor cartilage-meniscus and cartilage–synovial fluid contrast are the main reasons for the failure of automated software tools in segmenting cartilage for three-dimensional volume and thickness assessments that has been recently reported in OA patients [22]. The low prevalence of image artifacts and the substantially greater cartilage contrast afforded by two-dimensional FSE sequences suggest that a three-dimensional FSE imaging approach may have the potential to be relatively artifact free and to yield high image contrast and spatial resolution, essential prerequisites for accurate and reproducible visual and quantitative analysis of cartilage MR imaging.

Novel three-dimensional MR imaging pulse sequences

Three-dimensional driven equilibrium Fourier transform

A promising approach for imaging the patient with articular disorders is the DEFT technique [35–39]. Results of recent studies have shown that DEFT imaging provides contrast between cartilage and joint fluid by enhancing the signal from joint fluid, rather than by suppressing the signal from cartilage, as is the case with some sequences (Fig. 6).

DEFT produces image contrast that is a function of proton density, T1-T2, and TE-TR. The DEFT technique has been studied for many years, but so far has not been widely used. This is because T1 and T2 contrast compete in many tissues, so the T1-T2 DEFT

contrast tends to be flat. Fortunately, DEFT contrast is very well suited to imaging articular cartilage. Synovial fluid is high in signal intensity, and articular cartilage is intermediate in signal intensity. Bone appears low in signal intensity, and lipids are suppressed using a fat-saturation pulse. Hence, cartilage is easily distinguished from all of the adjacent tissues based on signal intensity alone, which greatly aids in segmentation and subsequent volume calculations.

Basic DEFT sequence includes a conventional spin echo pulse sequence followed by an additional refocusing pulse to form another echo, and then a reversed, excitation pulse to return any residual magnetization to the + z axis. This preserves the magnetization of the tissues that have longer T2, such as synovial fluid [35–39]. Three-dimensional DEFT

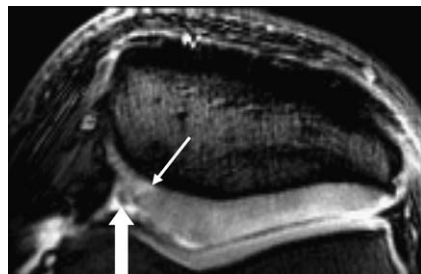


Fig. 6. Axial two-dimensional DEFT image through the patellofemoral articulation. The articular cartilage is well visualized. Joint fluid has high signal intensity. The thin arrow indicates a small cartilage fissure. The thick arrow indicates a cartilage flap arising from the fissure and extending into the fluid.

images with echo-planar readouts provide volumetric coverage in a clinically reasonable scan time and suggest that this sequence may be useful in clinical application (Fig. 7) [39].

The contrast-to-noise ratio efficiency between synovial fluid and cartilage has high values on fat-suppressed three-dimensional DEFT images. Fat-suppressed three-dimensional DEFT imaging is sensitive to signal intensity changes in degenerative cartilage.

Fat-suppressed three-dimensional DEFT imaging has several limitations. First, motion artifact is often seen, because of the longer scanning time than two-dimensional images and echo-planar imaging ghosts are seen because of the use of the echo-planar technique [35–39]. Second, for smaller field of view, stronger gradients are needed. Third, insufficient fat-suppression is often seen on fat-suppressed three-dimensional DEFT imaging, so further optimization may be necessary [39]. Finally, the areas of bone marrow edema are demonstrated as low or iso-signal intensity on fat-suppressed three-dimensional DEFT images, leading to underestimation of the extent of bone marrow edema [39]. Bone marrow edema is an important factor in diagnosis of OA. The complexity of signal intensity of bone marrow edema on fat-suppressed three-dimensional DEFT images seems to be caused by the fact that the contrast of DEFT imaging is dependent on the ratio T2-T1, not T1 or T2 relaxation times [39].

Water-excitation three-dimensional fast low-angle shot

Water-excitation three-dimensional fast low-angle shot is a sequence for faster imaging of articular

cartilage defects, compared with conventional fat saturation three-dimensional fast low-angle shot [75]. The principle of water-excitation sequences is the selective excitation of non-fat-bound protons. Time-consuming spectral fat saturation to eliminate fat signal is not necessary. This provides significant advantage of a reduced acquisition time and additionally obviates chemical-shift artifacts. The water-excitation three-dimensional fast low-angle shot sequence has been recently described to provide image quality comparable with fat saturation three-dimensional fast low-angle shot [75].

Three-dimensional steady-state free precession and multipoint fat-water separation

SSFP imaging is an efficient, high-signal method for obtaining three-dimensional MR images [41]. The SSFP sequence is a rapid gradient-echo MR imaging technique that can yield a superior SNR compared with other gradient-echo techniques (Fig. 8).

The three-dimensional SSFP sequence is a fully balanced steady-state coherent imaging pulse sequence designed to produce high SNR images at very short sequence times (TR). The pulse sequence uses fully balanced gradients to rephase the transverse magnetization at the end of each TR interval. To achieve fat saturation in a steady state, it is important to bring the magnetization back to the steady state as quickly as possible to avoid artifacts. A half-alpha technique is used to store magnetization and then return it to steady state relatively quickly. This is repeated throughout the sequence at regular intervals. The use of multiecho fat-water separation allows the use of small TE increments, and can be

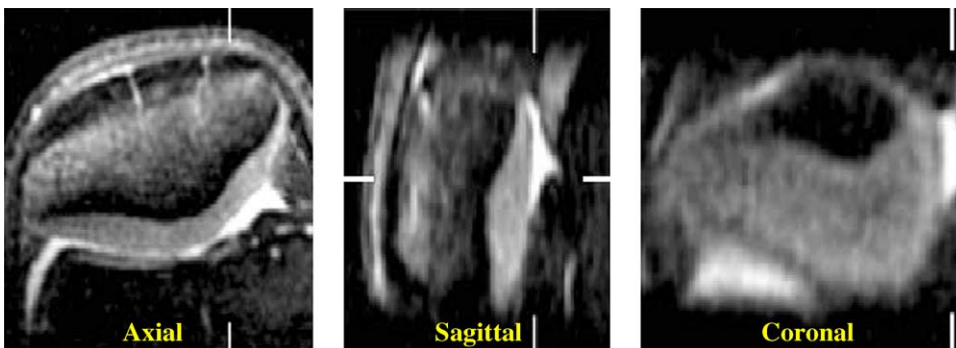


Fig. 7. Near isotropic three-dimensional DEFT acquisition using interleaved echoplanar acquisition. These images were obtained with the resolution of $0.5 \times 0.5 \times 1$ mm, a field of view of $13 \times 13 \times 13$ cm, and acquisition time of 11 minutes. The patellofemoral cartilage is demonstrated in the axial, sagittal, and coronal planes.



Fig. 8. Sagittal three-dimensional SSFP sequence obtained to the lateral tibiofemoral compartment (TR/TE/TI in milliseconds 6.6/1.2/20, flip angle 10° , 128 slices, 0.8-mm slice thickness, two excitations, matrix 256×256 , field of view 14 cm, acquisition time 8 minutes). The sequence provides near isotropic resolution. Cartilage signal is very high even compared with the surrounding tissues resulting in excellent contrast-to-noise ratio.

applied to three-dimensional SSFP imaging of articular cartilage imaging.

SSFP sequence has excellent contrast behavior with varying dependence on T1 and T2. Many different methods of SSFP-based imaging are available for imaging the articular cartilage, and all have higher cartilage signal compared with conventional techniques. Synovial fluid appears bright on SSFP images, because of its long T2.

With recent advances in MR imaging gradient hardware, it is now possible to use SSFP imaging without the limitations of banding or off-resonance artifacts. The best immunity to off-resonance artifacts when using SSFP [41], is a short repetition time (< 5 milliseconds). The major limitation of SSFP is image degradation caused by local magnetic field inhomogeneities if the TR is long.

Another similar approach that may provide more reliable fat suppression is Dixon SSFP imaging. This technique is faster and can provide more reliable fat suppression than fat-suppressed three-dimensional SPGR imaging. Dixon SSFP imaging may be especially useful at high field strength.

A final steady-state method of cartilage imaging that is useful at 3 T is SSFP imaging with intermittent fat saturation. This technique preserves the SNR advantage of SSFP imaging, but provides uniform fat saturation, even at high field strength. The overall SNR efficiency and speed of the SSFP-based techniques make them very attractive for cartilage imaging.

Three-dimensional fluctuating equilibrium MR imaging

Fluctuating equilibrium MR imaging [76,77] is a variant of SSFP imaging that may be useful in imaging cartilage in the knee [76]. In fluctuating equilibrium MR imaging, each phase-encoding step is repeated twice, once with a 90_x and once with a 90_y . The k-space data are then parsed to form two complete data sets, which are reconstructed into fat and water images. With a repetition time of 6.6 milliseconds, high-resolution three-dimensional imaging of cartilage is possible in about 2 minutes.

As with DEFT imaging, fluctuating equilibrium MR imaging produces contrast based on the ratio of T1-T2 in tissues. This results in bright fluid signal while preserving cartilage signal. The largest disadvantage of fluctuating equilibrium MR imaging and SSFP techniques is sensitivity to off-resonance artifacts [76].

Three-dimensional fast spin echo imaging

Standard two-dimensional FSE and three-dimensional SPGR sequences yield anisotropic voxels. Anisotropic voxels are difficult to process and can result in artifacts. Specifically, the poor slice profile, unwanted magnetization transfer effects, high-power deposition, or poor SNR of conventional two-dimensional slice-selective and multislab three-dimensional MR imaging methods can cause problems. A single-slab three-dimensional FSE sequence has been developed by the University of Virginia at Arlington and Brigham and Women's Hospital for neuroimaging [20,78] and has been tested to obtain high-resolution images of the brain [20] and petrous bone [21]. Images in these studies have near-isotropic voxel sizes of $0.4 \times 0.4 \times 0.6 \text{ mm}^3$, which allows one to use isotropic image processing techniques without introducing significant artifacts.

The novel three-dimensional FSE sequence uses a single-slab technique with hard pulses for the excitation and for the refocusing radiofrequency pulses. This results in very small effective echo time and echo spacing. The novel three-dimensional FSE sequence differs from the product sequences of major MR imaging companies in many aspects. First, it has single-slab coverage for the whole field of view, whereas many product sequences are multislab because of the long sequence time needed. Single-slab three-dimensional MR imaging gives high SNR and eliminates unwanted magnetization transfer and boundary image artifacts. Second, the

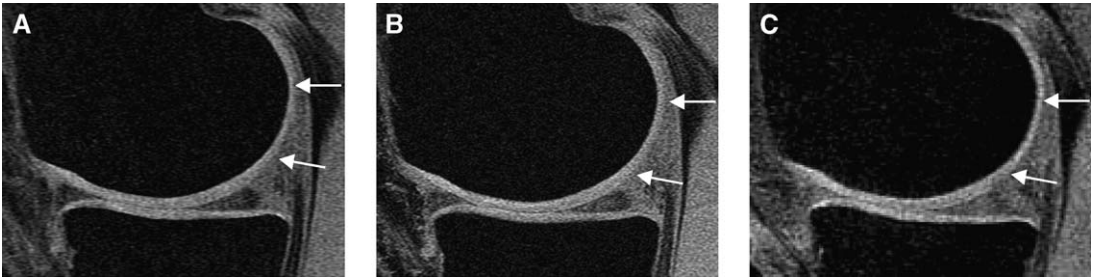


Fig. 9. Comparison of three-dimensional SPGR, three-dimensional SS-SPGR (water selective excitation gradient echo), and three-dimensional FSE images. Three-dimensional SPGR (A), three-dimensional SS-SPGR (B), and three-dimensional FSE images (C). Contrast between cartilage and posterior capsule (arrows) is best in this patient with three-dimensional FSE. This is a problem area for automated or semiautomated segmentation of cartilage for subsequent quantitative analysis, such as measurements of volume and thickness. Blurring is not a problem with this sequence because of its short echo times.

sequence uses hard excitation and refocusing radio-frequency pulses that can significantly reduce echo spacing compared with the conventional soft pulse approach. This greatly helps to reduce the effective echo time in T1-weighted imaging and helps to reduce the echo train length that shortens the total scan time and eliminates image artifacts caused by signal quick decaying. Third, dynamic receiver gains can be implemented during three-dimensional data

acquisition, which improves SNR compared with the conventional single gain approach. A twofold to threefold SNR gain can be obtained with this approach [20].

Three-dimensional FSE provides image contrast similar to the one experienced with routinely used two-dimensional FSE sequences (Fig. 9). The sequence can provide isotropic image resolution. In the future, this may create the opportunity of single-

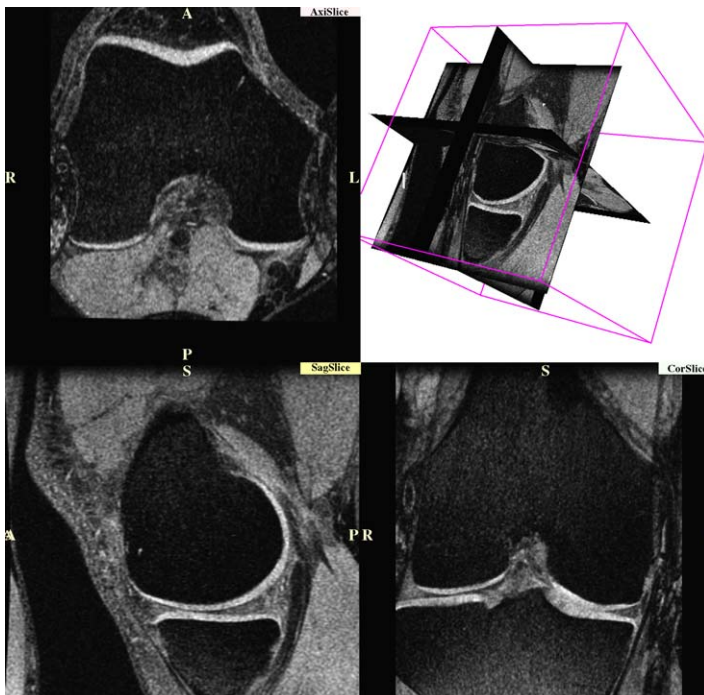


Fig. 10. Simultaneous multiplanar display of three-dimensional FSE images, 3-T MR image. The three-dimensional FSE sequence is acquired with near isotropic resolution ($0.47 \times 0.6 \times 0.5$ mm). Images can be displayed in any desired plane without apparent loss in image quality. Partial volume artifacts are greatly reduced using this approach.

pulse sequence knee MR imaging with isotropic resolution; in this setting, the radiologist can rotate and review the acquisition in any desired orientation without loss of spatial resolution (Fig. 10).

Acknowledgments

The authors would like to thank Inez Wu for assistance in preparing the manuscript.

References

- [1] Doherty M, Hutton C, Bayliss MT. Osteoarthritis. In: Maddison PJ, et al, editors. Oxford textbook of rheumatology. Oxford: Oxford University Press; 1993. p. 959–83.
- [2] Brittberg M, Lindahl A, Nilsson A, et al. Treatment of deep cartilage defects in the knee with autologous chondrocyte transplantation. *N Engl J Med* 1994; 331:889–95.
- [3] Brittberg M, Lindahl A, Homminga G, et al. A critical analysis of cartilage repair. *Acta Orthop Scand* 1997;68:186–91.
- [4] Garrett JC. Osteochondral allografts for reconstruction of articular defects of the knee. *Instr Course Lect* 1998; 47:517–22.
- [5] Stevenson S, Dannucci GA, Sharkey NA, et al. The fate of articular cartilage after transplantation of fresh and cryopreserved tissue-antigen-matched and mismatched osteochondral allografts in dogs. *J Bone Joint Surg* 1989;71:1297–307.
- [6] Bobic V. Arthroscopic osteochondral autograft transplantation in anterior cruciate ligament reconstruction: a preliminary clinical study. *Knee Surg Sports Traumatol Arthrosc* 1996;3:262–4.
- [7] Buckland-Wright JC, Macfarlane DG, Williams SA, et al. Accuracy and precision of joint space width measurements in standard and macroradiographs of osteoarthritic knees. *Ann Rheum Dis* 1995;54:872–80.
- [8] Buckland-Wright JC, Wolfe F, Ward RJ, et al. Substantial superiority of semiflexed (MTP) views in knee osteoarthritis: a comparative radiographic study, without fluoroscopy, of standing extended, semiflexed (MTP), and schuss views. *J Rheumatol* 1999;26: 2664–74.
- [9] Burgkart R, Glaser C, Hyhlik-Durr A, et al. Magnetic resonance imaging-based assessment of cartilage loss in severe osteoarthritis: accuracy, precision, and diagnostic value. *Arthritis Rheum* 2001;44:2072–7.
- [10] Disler DG, McCauley TR, Wirth CR, et al. Detection of knee hyaline cartilage defects using fat-suppressed three-dimensional spoiled gradient-echo MR imaging: comparison with standard MR imaging and correlation with arthroscopy. *AJR Am J Roentgenol* 1995;165: 377–82.
- [11] Disler DG, McCauley TR, Kelman CG, et al. Fat-suppressed three-dimensional spoiled gradient-echo MR imaging of hyaline cartilage defects in the knee: comparison with standard MR imaging and arthroscopy. *AJR Am J Roentgenol* 1996;167:127–32.
- [12] Disler DG. Fat-suppressed three-dimensional spoiled gradient recalled MR imaging: assessment of articular and physal hyaline cartilage. *AJR Am J Roentgenol* 1997;169:1117–23.
- [13] Potter HG, Linklater JM, Allen AA, et al. Magnetic resonance imaging of articular cartilage in the knee: an evaluation with use of fast-spin-echo imaging. *J Bone Joint Surg Am* 1998;80:1276–84.
- [14] McCauley TR, Kier R, Lynch KJ, et al. Chondromalacia patellae: diagnosis with MR imaging. *AJR Am J Roentgenol* 1992;158:101–5.
- [15] Peterfy CG, van Dijke CF, Janzen DL, et al. Quantification of articular cartilage in the knee with pulsed saturation transfer subtraction and fat-suppressed MR imaging: optimization and validation. *Radiology* 1994; 192:485–91.
- [16] Peterfy CG, Majumdar S, Lang P, et al. MR imaging of the arthritic knee: improved discrimination of cartilage, synovium, and effusion with pulsed saturation transfer and fat-suppressed T1-weighted sequences. *Radiology* 1994;191:413–9.
- [17] Broderick LS, Turner DA, Renfrew DL, et al. Severity of articular cartilage abnormality in patients with osteoarthritis: evaluation with fast spin-echo MR vs arthroscopy. *AJR Am J Roentgenol* 1994;162:99–103.
- [18] Recht MP, Piraino DW, Paletta GA, et al. Accuracy of fat-suppressed three-dimensional spoiled gradient-echo FLASH MR imaging in the detection of patellofemoral articular cartilage abnormalities. *Radiology* 1996;198: 209–12.
- [19] Yoshioka H, Stevens K, Genovese M, et al. Articular cartilage of knee: normal patterns at MR imaging that mimic disease in healthy subjects and patients with osteoarthritis. *Radiology* 2004;231:31–8.
- [20] Zhao L, et al. A high-resolution clinical whole-brain scan using single-slab three-dimensional T1W, T2W and FLAIR fast spin-echo sequences. In: Proceedings of the International Society of Magnetic Resonance in Medicine. Honolulu, Hawaii, May, 2002. p. 1294.
- [21] Zhao L, Bartling S, Mugler J, et al. High-resolution MR imaging of the petrous bone using a single-slab three-dimensional T2-weighted fast spin-echo sequence. In: Proceedings of the International Society of Magnetic Resonance in Medicine. Honolulu, Hawaii, May, 2002. p. 312.
- [22] Gandy SJ, Dieppe PA, Keen MC, et al. No loss of cartilage volume over three years in patients with knee osteoarthritis as assessed by magnetic resonance imaging. *Osteoarthritis Cartilage* 2002;10:929–37.
- [23] Conway WF, Hayes CW, Loughran T, et al. Cross-sectional imaging of the patellofemoral joint and surrounding structures. *Radiographics* 1991;11:195–217.
- [24] Hayes C, Sawyer R, Conway W. Patellar cartilage lesions: in vitro detection and staging with MR imag-

- ing and pathologic correlation. *Radiology* 1990;176:763-6.
- [25] Karvonen RL, Negendank WG, Fraser SM, et al. Articular cartilage defects of the knee: correlation between magnetic resonance imaging and gross pathology. *Ann Rheum Dis* 1990;49:672-5.
- [26] Recht MP, Resnick D. MR imaging of articular cartilage: current status and future directions. *AJR Am J Roentgenol* 1994;163:283-90.
- [27] Recht MP, Kramer J, Marcelis S, et al. Abnormalities of articular cartilage in the knee: analysis of available MR techniques. *Radiology* 1993;187:473-8.
- [28] Yulish BS, Montanez J, Goodfellow DB, et al. Chondromalacia patellae: assessment with MR imaging. *Radiology* 1987;164:763-6.
- [29] Lehner KB, et al. Structure, function, and degeneration of bovine hyaline cartilage: assessment with MR imaging in vitro. *Radiology* 1989;170:495-9.
- [30] Henkelman RM, Stanisz GJ, Kim JK, et al. Anisotropy of NMR properties of tissues. *Magn Reson Med* 1994;32:592-601.
- [31] Woolf SD, et al. Magnetization transfer contrast: MR imaging of the knee. *Radiology* 1991;179:623-8.
- [32] Pauly JM, et al. Slice selective excitation for very short T2 species. In: *Society for Magnetic Resonance in Medicine: book of abstracts*; 1990.
- [33] Brossmann J, et al. Short echo time projection reconstruction MR imaging of cartilage: comparison with fat-suppressed spoiled GRASS and magnetization transfer contrast MR imaging. *Radiology* 1997;203:501-7.
- [34] Gold G, Pauly JM, Macovski A, et al. MR spectroscopic imaging of collagen: tendons and knee menisci. *Magn Reson Med* 1995;34:647-54.
- [35] Hargreaves BA, et al. Comparison of novel sequences for imaging articular cartilage. In: *Proceedings of the International Society of Magnetic Resonance in Medicine*; 2002.
- [36] Hargreaves BA, et al. Technical considerations for DEFT imaging. In: *International Society for Magnetic Resonance in Medicine*. Sydney, Australia; 1998.
- [37] Hargreaves BA, et al. Imaging of articular cartilage using driven equilibrium. In: *International Society for Magnetic Resonance in Medicine*. Sydney, Australia; 1998.
- [38] Hargreaves BA, Gold GE, Lang PK, et al. MR imaging of articular cartilage using driven equilibrium. *Magn Reson Med* 1999;42:695-703.
- [39] Yoshioka H, Stevens K, Hargreaves BA, et al. Magnetic resonance imaging of articular cartilage of the knee: comparison between fat-suppressed three-dimensional SPGR imaging, fat-suppressed FSE imaging, and fat-suppressed three-dimensional DEFT imaging, and correlation with arthroscopy. *J Magn Reson Imaging* 2004;20:857-64.
- [40] Yoshioka H, Alley M, Steines D, et al. Imaging of the articular cartilage in osteoarthritis of the knee joint: 3D spatial-spectral spoiled gradient-echo versus fat-suppressed 3D spoiled gradient-echo MR imaging. *J Magn Reson Imaging* 2003;18:66-71.
- [41] Reeder SB, Pelc NJ, Alley MT, et al. Rapid MR imaging of articular cartilage with steady-state free precession and multipoint fat-water separation. *AJR Am J Roentgenol* 2003;180:357-62.
- [42] Lang P, et al. Cartilage MR imaging at 3.0T: comparison of 3D SPGR, 3D MFAST and 3D FSE sequences. In: *OARSI Omeract Workshop for Consensus in Osteoarthritis Imaging*. Bethesda, Maryland; 2002.
- [43] Bredella MA, Tirman PF, Peterfy CG, et al. Accuracy of T2-weighted fast spin-echo MR imaging with fat saturation in detecting cartilage defects in the knee: comparison with arthroscopy in 130 patients. *AJR Am J Roentgenol* 1999;172:1073-80.
- [44] Kawahara Y, Uetani M, Nakahara N, et al. Fast spin-echo MR of the articular cartilage in the osteoarthrotic knee: correlation of MR and arthroscopic findings. *Acta Radiol* 1998;39:120-5.
- [45] McNicholas MJ, Brooksbank AJ, Walker CM. Observer agreement analysis of MRI grading of knee osteoarthritis. *J R Coll Surg Edinb* 1999;167:757-60.
- [46] Eckstein F, Gavazzeni A, Sittek H, et al. Determination of knee joint cartilage thickness using three-dimensional magnetic resonance chondro-crassometry (3D MR-CCM). *Magn Reson Med* 1996;36:256-65.
- [47] Eckstein F, Sittek H, Gavazzeni A, et al. Magnetic resonance chondro-crassometry (MR CCM): a method for accurate determination of articular cartilage thickness? *Magn Reson Med* 1996;35:89-96.
- [48] Eckstein F, Westhoff J, Sittek H, et al. In vivo reproducibility of three-dimensional cartilage volume and thickness measurements with MR imaging. *AJR Am J Roentgenol* 1998;170:593-7.
- [49] Stammberger T, Hohe J, Englmeier KH, et al. Patellofemoral joint cartilage thickness and contact areas from MRI in patients with osteoarthritis. In: *International Society for Magnetic Resonance in Medicine*. Sydney, Australia; 1998.
- [50] Stammberger T, Eckstein F, Englmeier KH, et al. Determination of 3D cartilage thickness data from MR imaging: computational method and reproducibility in the living. *Magn Reson Med* 1999;41:529-36.
- [51] Tieschky M, Faber S, Haubner M, et al. Repeatability of patellar cartilage thickness patterns in the living, using a fat-suppressed magnetic resonance imaging sequence with short acquisition time and three-dimensional data processing. *J Orthop Res* 1997;15:808-13.
- [52] Peterfy C, van Dijke CF, Lu Y, et al. Quantification of the volume of articular cartilage in the metacarpophalangeal joints of the hand: accuracy and precision of three-dimensional MR imaging. *AJR Am J Roentgenol* 1995;165:371-5.
- [53] Piplani MA, Disler DG, McCauley TR, et al. Articular cartilage volume in the knee: semiautomated determination from three-dimensional reformations of MR images. *Radiology* 1996;198:855-9.
- [54] Steines D, Napel S, Lang P. Measuring volume of articular cartilage defects in osteoarthritis using MRI: validation of a new method. In: *Radiological Society of North America*. Chicago, Illinois, December, 2000.

- [55] Steines D, Napel S, Lang P, et al. Segmentation of osteoarthritic femoral cartilage using live wire. Presented at the ISMRM Eighth Scientific Meeting, Denver, Colorado, 2000.
- [56] Stammberger T, Eckstein F, Michaelis M, et al. Interobserver reproducibility of quantitative cartilage measurements: comparison of B-spline snakes and manual segmentation. *Magn Reson Imaging* 1999;17:1033–42.
- [57] Warfield S, Winalski C, Jolesz F, et al. Automatic segmentation of MRI of the knee. In: *International Society for Magnetic Resonance in Medicine*. Sydney, Australia, April, 1998. p. 563.
- [58] Pilch L, Stewart C, Gordon D, et al. Assessment of cartilage volume in the femorotibial joint with magnetic resonance imaging and 3D computer reconstruction. *J Rheumatol* 1994;21:2307–21.
- [59] Hardy PA, Nammalwar P, Kuo S. Measuring the thickness of articular cartilage from MR images. *J Magn Reson Imaging* 2001;13:120–6.
- [60] Hardya PA, Newmark R, Liu YM, et al. The influence of the resolution and contrast on measuring the articular cartilage volume in magnetic resonance images. *Magn Reson Imaging* 2000;18:965–72.
- [61] Westin CF, Wigstrom L, Looock T, et al. Three-dimensional adaptive filtering in magnetic resonance angiography. *J Magn Reson Imaging* 2001;14:63–71.
- [62] Westin CF, Richolt J, Moharir V, et al. Affine adaptive filtering of CT data. *Med Image Anal* 2000;4:161–77.
- [63] Rodrigues-Florido MA, Krissian K, Ruiz-Alzola J, et al. Comparison of two restoration techniques in the context of 3D medical imaging. In: *MICCAI 2000: Fourth International Conference on Medical Image Computing and Computer-Assisted Intervention*. Utrecht, The Netherlands: Springer Verlag; 2000.
- [64] Sijbers J, Scheunders P, Verhoye M, et al. Watershed-based segmentation of 3D MR data for volume quantization. *Magn Reson Imaging* 1997;15:679–88.
- [65] Falcão AX, Udupa JK. Segmentation of 3D objects using live wire. In: *SPIE Medical Imaging*. Newport Beach, California. 1997;3024:25.
- [66] Falcão AX, Udupa JK. User-steered image segmentation paradigms: live wire and live lane. *GMIP* 1998;60:233–60.
- [67] Warfield SK, Kaus M, Jolesz FA, et al. Adaptive, template moderated, spatially varying statistical classification. *Med Image Anal* 2000;4:43–55.
- [68] Warfield S, Dengler J, Zaers J, et al. Automatic identification of gray matter structures from MRI to improve the segmentation of white matter lesions. *J Image Guid Surg* 1995;1:326–38.
- [69] Iosifescu DV, Shenton ME, Warfield SK, et al. An automated registration algorithm for measuring MRI subcortical brain structures. *Neuroimage* 1997;6:13–25.
- [70] Eckstein F, Heudorfer L, Faber SC, et al. Long-term and resegmentation precision of quantitative cartilage MR imaging (qMRI). *Osteoarthritis Cartilage* 2002;10:922–8.
- [71] Glaser C, Faber S, Eckstein F, et al. Optimization and validation of a rapid high-resolution T1-w 3D FLASH water excitation MRI sequence for the quantitative assessment of articular cartilage volume and thickness. *Magn Reson Imaging* 2001;19:177–85.
- [72] Wluka AE, Stuckey S, Snaddon J, et al. The determinants of change in tibial cartilage volume in osteoarthritic knees. *Arthritis Rheum* 2002;46:2065–72.
- [73] Gandy SJ, Brett AD, Pirppe PA, et al. No apparent progressive change to knee cartilage volumes over one year in rheumatoid and osteoarthritis. In: *Proceedings of the International Society of Magnetic Resonance in Medicine*. Denver, Colorado, (CO); 2000.
- [74] Kellgren J, Lawrence J. Radiological assessment of osteoarthritis. *Ann Rheum Dis* 1957;16:494–501.
- [75] Hyhlik-Durr A, Faber S, Burgkart R, et al. Precision of tibial cartilage morphometry with a coronal water-excitation MR sequence. *Eur Radiol* 2000;10:297–303.
- [76] Vasnawala SS, Pauly JM, Nishimura DG, et al. MR imaging of knee cartilage with FEMR. *Skeletal Radiol* 2002;31:574–80.
- [77] Vasanawala SS, Pauly JM, Nishimura DG. Fluctuating equilibrium MRI. *Magn Reson Med* 1999;42:876–83.
- [78] Mugler III JP, Bao S, Mulkern RV, et al. Optimized single-slab three-dimensional spin-echo MR imaging of the brain. *Radiology* 2000;216:891–9.